

# Design, Fabrication, and Persistent Current Operation of the REBCO Floating Coil for the Plasma Experimental Device Mini-RT

Yuichi OGAWA, Junji MORIKAWA, Kenichiro UCHIJIMA, Yuichiro HOSAKA, Chika KAWAI, Kenzo IBANO, Toshiyuki MITO<sup>1)</sup>, Nagato YANAGI<sup>1)</sup>, Kyohhei NATSUME<sup>1)</sup>, Yoshiro TERAZAKI<sup>2)</sup>, Masataka IWAKUMA<sup>3)</sup>, Akira TOMIOKA<sup>4)</sup> and Shinichi NOSE<sup>4)</sup>

*Graduate School of Frontier Sciences, University of Tokyo, Kashiwa 277-8568, Japan*

<sup>1)</sup>*National Institute for Fusion Science, Toki, Gifu 509-5292, Japan*

<sup>2)</sup>*Graduate University for Advanced Studies, Toki, Gifu 509-5292, Japan*

<sup>3)</sup>*Graduate School of Information Science and Electrical Engineering, Kyushu University, Fukuoka 819-0395, Japan*

<sup>4)</sup>*Fuji Electric Co., Ltd., Ichihara, Chiba 290-8511, Japan*

(Received 21 October 2013 / Accepted 18 December 2013)

High-temperature superconductor technology has become remarkably advanced, and components such as current leads and magnets have been explored for their applicability to fusion. Especially, REBa<sub>2</sub>Cu<sub>3</sub>O<sub>7-δ</sub> (RE = rare-earth: REBCO) tape has been developed in research fields other than fusion, because of superior performance of REBCO in high magnetic fields. Here, we fabricated a REBCO coil with a radius of 150 mm and a total coil current of 55.2 kA, to be applied as an internal floating coil in Mini-RT, a plasma experimental device. This newly fabricated REBCO coil has replaced the Bi<sub>2</sub>Sr<sub>2</sub>Ca<sub>2</sub>Cu<sub>3</sub>O<sub>10</sub> (BSCCO) coil developed in 2003, and has improved coil performance and plasma operation. A REBCO tape of width 4.3 mm was employed, and a 0.1 mm-thick copper laminate was attached for the countermeasure at the quench. In addition, the REBCO tape was wrapped in a polyimide sheet for electric insulation, increasing the total thickness of the REBCO tape to 0.27–0.28 mm. A persistent current switch was constructed from a small-turn REBCO winding with a heater formed from a stainless steel sheet. Solder joint of two REBCO tapes over a 30 mm length were employed, by overlapping their copper laminates. Persistent current, with a decay time ~320 h, has been successfully achieved at 25 K operation temperature. This decay time corresponds to a resistance of ~125 nΩ, roughly consistent with the total resistance of the seven joint sections in the persistent current circuit.

© 2014 The Japan Society of Plasma Science and Nuclear Fusion Research

Keywords: High Temperature Superconductor (HTS), REBCO tape, persistent current, Persistent Current Switch (PCS), internal floating coil

DOI: 10.1585/pfr.9.1405014

## 1. Introduction

High temperature superconductors (HTSs) are extensively used in electrical components such as power cables and electric transformers. Initially, BSCCO tapes were employed in these applications, because a relatively long tape with a high critical current was available. We developed a BSCCO coil for the plasma experimental device Mini-RT [1–9], in which a high-temperature plasma is confined within a dipole magnetic field. The field is produced by an internal floating coil constructed from a BSCCO tape, and this represents the first application of an HTS coil to plasma experimental devices. The BSCCO coil in the Mini-RT device operates in a persistent current mode. Since current is excited by an external power supply, a persistent current switch (PCS) is installed in the internal coil. The decay time of the persistent current was ~20 h at  $I_{op} = 100$  A and  $T_{op} = 21$  K [4]. During 10 years

of operation, the decay time of the persistent current has gradually decreased to ~2.7 h. This deterioration of the persistent current has become problematic for plasma experiments, which require a constant magnetic field for several hours.

Here we should remark that the BSCCO tape has been remarkably improved by introducing a controlled over pressure (CT-OP<sup>TM</sup>) sintering furnace in 2004 [10], and since then the improved tape, called the Dramatically Innovative-(DI-) BSCCO tape, has been available in the market. While, before the development of this high-performance DI-BSCCO tape, the BSCCO coil, which is used in the Mini-RT device, was fabricated in 2003.

REBCO tape technology has considerably advanced in recent years, and REBCO tapes longer than a few hundred meters are now available. In addition, since a winding technique for REBCO coils has been developed, REBCO coils have been applied in numerous fields. Of particular

author's e-mail: ogawa@ppl.k.u-tokyo.ac.jp

interest and importance in some fields is the development of a REBCO coil operating in persistent current mode. In this study, we have decided to replace the BSCCO coil in the Mini-RT device with a newly fabricated REBCO coil.

This manuscript is organized as follows. Section 2 presents the design and fabrication of the REBCO coil for the Mini-RT device. The results of cooling and excitation experiments are given in Sec. 3. Finally, the summary is presented in Sec. 4.

## 2. Design and Fabrication of a REBCO Coil for the Mini-RT Device

In 2003, the Mini-RT device was constructed for the study of high-beta plasmas in an advanced fusion plasma confinement. In this device, high-temperature plasma is confined by the dipole magnetic field produced by the levitated internal coil. Previous internal coil devices such as Spherator and Levitron were constructed using low-temperature superconductors [11, 12]. The Mini-RT was the first application of HTS in fusion plasma devices.

An elevation view of the Mini-RT device and the cross section of the plasma confinement region are shown in Fig. 1. Initially, the internal coil is cooled and excited at the basal region of the vacuum vessel, and a persistent current is established. Demountable transfer tubes are inserted into the internal coil, by which the internal coil is cooled with cold He gas supplied by Gifford–McMahon (GM) refrigerators. Next, two electrodes are connected to sockets installed within the internal coil, and the coil current is excited by the external power supply. Persistent current mode is established by the persistent current switch, also

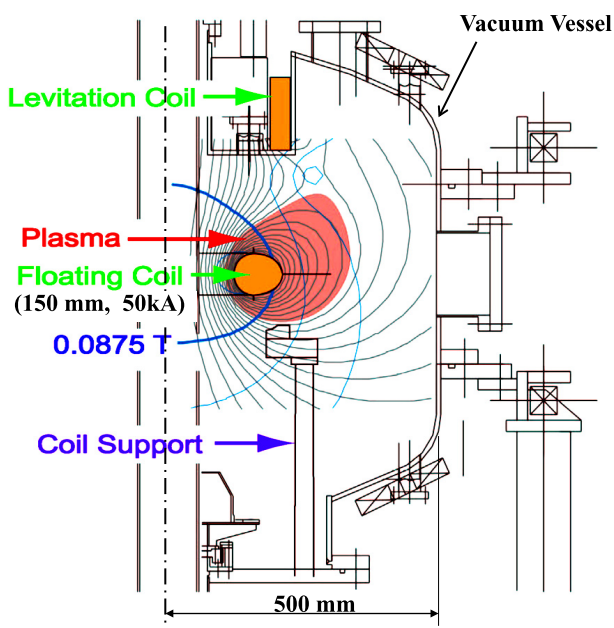


Fig. 1 Elevation view of the Mini-RT device, and cross section of the plasma.

installed inside the internal coil. Since the internal coil is disconnected from the cooling system during plasma experiments, its temperature gradually increases, limiting its operational time during plasma experiments.

While operating in persistent current mode, the internal coil is mechanically lifted into the mid-plane of the vacuum vessel, and is suspended by exciting the levitation coil located at the top of the vacuum vessel. Since the magnetically levitated internal coil is vertically unstable, the levitation coil current is feed-back controlled by measuring the internal coil position with laser sensors. We have successfully levitated the internal coil during a few hours with an accuracy of 0.1 mm.

The cross section of the internal coil is shown in Fig. 2, where the main coil and PCS are covered with a thermal shield made from copper. The main coil was layer-wound and cooled with cold He gas, flowing through a cooling pipe attached to the coil frame. The PCS comprises a REBCO winding with a bifilar method and a co-wound stainless steel heater. The PCS switches as the REBCO winding conditions between superconducting and normal by controlling the PCS temperature with the heater. The egg-shaped coil casing of the internal coil contains the check valves and electrode sockets. In this study, we have replaced the main coil and PCS made from BSCCO tape with those constructed from REBCO; however, other components such as thermal shield, check-valves, and electrode sockets of electrodes have been reused.

### 2.1 Characteristics of REBCO tape

The specifications of the REBCO tape employed in the Mini-RT coil are listed in Table 1. Because the winding pack for the main coil (Fig. 2) is size-restricted, the REBCO tape could not be larger than the original BSCCO tape. Thus, we cut the original 10 mm-wide REBCO tape into 4.32 mm width. Since the Mini-RT coil required more

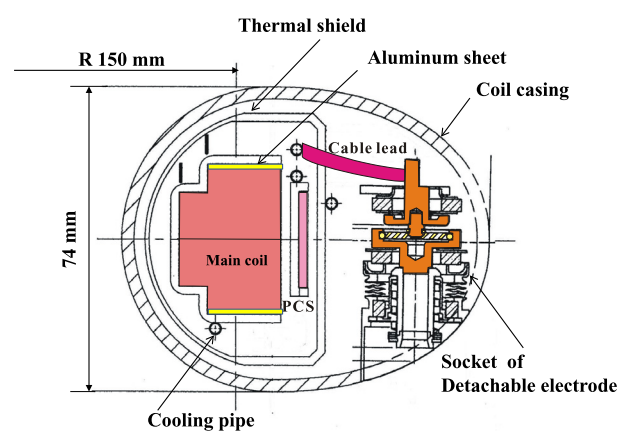


Fig. 2 Cross section of the Mini-RT internal floating coil. A REBCO tape is employed for the main coil and the PCS, and an aluminum sheet is inserted between the winding pack and the coil frame.

Table 1 Specifications of REBCO tapes employed in the main coil.

	No. 1 tape	No. 2 tape
Polyimide tape	49.6 $\mu\text{m}$ (12.4 $\mu\text{m} \times 4$ )	50.0 $\mu\text{m}$ (12.5 $\mu\text{m} \times 4$ )
Copper: Cu	100 $\mu\text{m}$	100 $\mu\text{m}$
Tin: Sn	2 - 4 $\mu\text{m}$	2 - 4 $\mu\text{m}$
Silver: Ag	6.5 $\mu\text{m}$	5.1 $\mu\text{m}$
REBCO	2.3 $\mu\text{m}$	3.1 $\mu\text{m}$
CeO <sub>2</sub>	0.4 $\mu\text{m}$	0.4 $\mu\text{m}$
MgO	5 nm	5 nm
Y <sub>2</sub> O <sub>3</sub>	25 nm	25 nm
Al <sub>2</sub> O <sub>3</sub>	100 nm	100 nm
Hastelloy	100 $\mu\text{m}$	100 $\mu\text{m}$

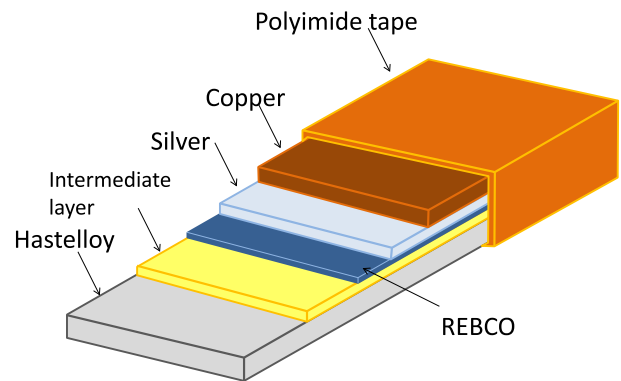
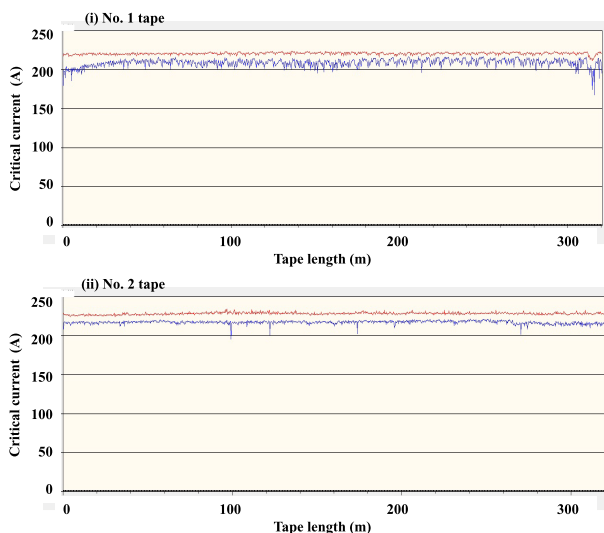


Fig. 4 Schematic of the REBCO tape prepared for the Mini-RT coil. A REBCO tape with a copper laminate is wrapped within a polyimide sheet. The REBCO tape is 4.32 mm wide, and its total thickness is 0.27 - 0.28 mm.


 Fig. 3 Critical current,  $I_c$ , of two REBCO tapes employed in the Mini-RT coil, measured at 77 K under the self-magnetic field condition and an induced voltage of 1  $\mu\text{V}/\text{cm}$ . Since signals measured by a Hall sensor fluctuate, the upper and lower bounds of the measured signals are depicted as red and blue lines, respectively. The width of the REBCO tape is 4.32 mm. The end regions of tape No.1 were not used because the critical current degraded at the end regions.

than 500 m of tape, we used two segments of REBCO tapes, each exceeding 300 m in length. As shown in Fig. 3, measurements revealed that the critical current exceeds 200 A (77 K, self-field, 1  $\mu\text{V}/\text{cm}$ ) in almost all regions of the 300-m tape.

The REBCO tape substrate was a Hastelloy of 0.1-mm thickness. To overcome the poor electric and heat conductivities of the Hastelloy substrate, the REBCO tape was affixed with a 0.1 mm-thick copper laminate. The thickness of the copper laminate was determined by the countermea-

sure on the quench of the REBCO layer, as discussed later. In addition, the REBCO tape was electrically insulated by a polyimide sheet, as shown in Fig. 4. The total thickness of the REBCO tape was, resultantly, 0.27 - 0.28 mm.

## 2.2 Design of main coil with a REBCO tape

For comparison, the specifications of the main coil wound with the REBCO tape, and those of the BSCCO-based coil are summarized in Table 2. The major radius of the Mini-RT coil is 150 mm. As discussed in the previous section, the REBCO and BSCCO tapes were of equal width, and the main coil was fabricated with a layer-winding method. To reinforce the winding pack of the main coil, epoxy resin was applied on the REBCO tape under atmospheric conditions during the winding process. Since the total thickness of the REBCO tape is reduced (i.e., 0.27 - 0.28 mm in REBCO tape, and 0.39 mm in BSCCO one), we successfully increased the turn number of the main coil wound with REBCO tape by 30% rather than that with the BSCCO tape. The inductance of the REBCO coil is increased to be 0.144 H.

The rated operation current,  $I_{op}$ , of the REBCO tape is 100 A, yielding a total coil current of 55.2 kA, and a total stored magnetic energy of 0.72 kJ. The distribution of the magnetic field is shown in Fig. 5. This figure presents the magnetic field perpendicular to the REBCO tape, which is maximized at 0.656 T in the top/bottom areas of the winding pack.

Thermal quench of the REBCO coil is of major concern during persistent current operation. Since the spread of hot-spot heat along the REBCO tape is not easily estimated, we calculated the temperature increase as a function of the REBCO tape length transiting to the normal state. From the results, which are plotted in Fig. 6, we observe that the increase in temperature depends on the tape length of the normal zone. For example, if the tape length of the normal state is below 0.5 m, the temperature of the RE-

Table 2 Specification of main coils made from BSCCO and REBCO tapes, installed in the Mini-RT device. The BSCCO coil fabricated in 2003 was recently replaced by the REBCO coil.

	BSCCO coil	REBCO coil
Fabrication year	2003	2013
Major radius	150 mm	149.3 mm
Minor radius	16.15 mm	16.04 mm
Total coil current	50,000 A	55,200 A
Super conductor	Bi-2223	REBCO
vendor	Sumitomo	Fujikura
Cross section of a tape		
Width	4.4 mm	4.36 mm
Thickness	0.39 mm	0.272 - 0.281 mm
stabilizer	Silver ratio = 1.57	0.1-mm thick Copper laminate
Critical current: $I_c$ at 77K, self field, $1 \mu\text{V}/\text{cm}$	$\sim 100$ A	216 - 223 A
Critical temperature: $T_c$	$\sim 113$ K	92 K
Operation current: $I_{op}$	116.82 A	100 A
Coil turns	428	552
Current density	$64.95 \text{ A}/\text{mm}^2$	$68.30 \text{ A}/\text{mm}^2$
Total tape length	403.4 m	517 m
Winding/bonding	Layer winding/epoxy resin	
Coil inductance	0.0876 H	0.144 H
Stored magnetic energy	0.598 kJ	0.720 kJ
Magnetic field strength		
$B_r$ : radial component	0.6043 T	0.656 T
$B_z$ : perpendicular component	0.7944 T	0.841 T

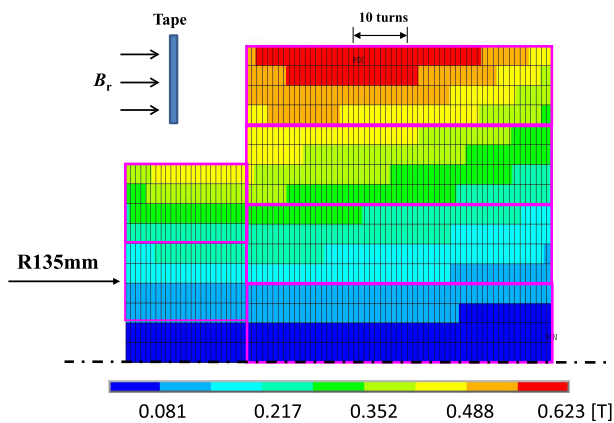


Fig. 5 Distribution of the magnetic field strength perpendicular to the REBCO tape at a total coil current of 55.2 kA. In the figure, upper half of the winding pack is shown. The maximum magnetic field perpendicular to the tape appears at the top/bottom of the winding pack.

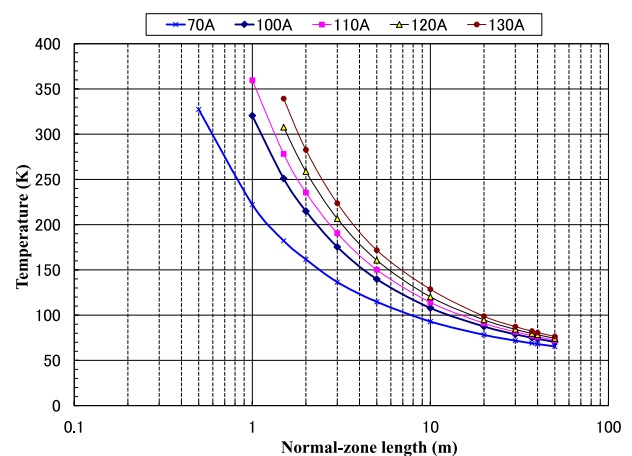


Fig. 6 Temperature increase at the quench of the main coil, as a function of tape length transitioned from the super to normal conducting state for various operational coil currents. The initial coil temperature is assumed as 50 K.

BCO tape might increase to 320 K even when  $I_{op} = 70$  A. The temporal evolution of the coil temperature, shown in Fig. 7 (a), indicates that 300 K is reached in around 20 s. When  $I_{op} = 130$  A, to maintain an acceptable temperature increase, more than a few meters of tape length should transit to the normal state. Figure 7 (b) shows the temporal

evolution of the coil temperature, coil current, and induced voltage in the coil at  $I_{op} = 130$  A and 10 m of tape in the normal state. Although the temperature is restrained at a sufficiently low level (i.e.,  $\sim 130$  K), the voltage induced in the coil by the large resistance of the circuit requires at-

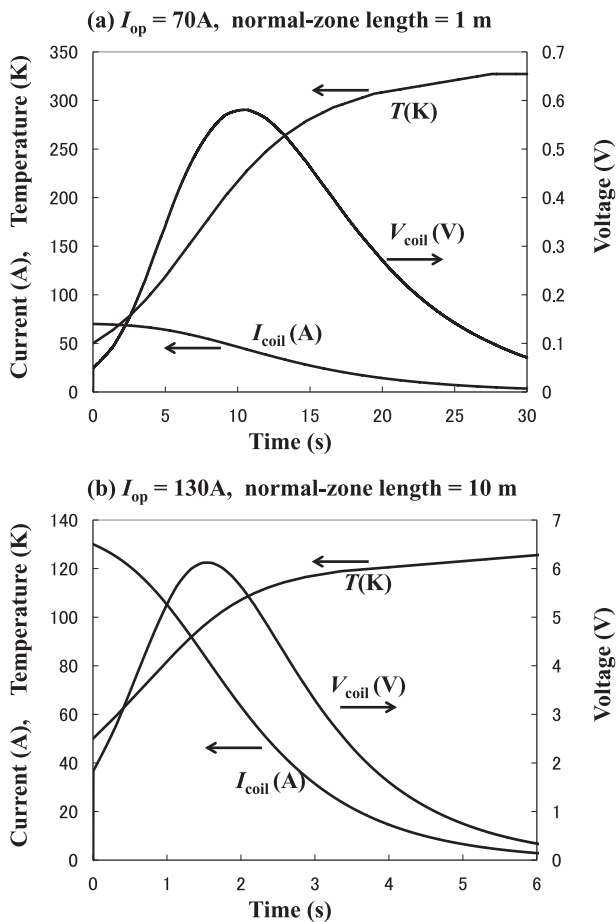


Fig. 7 Time evolutions of the coil current, temperature, and voltage at the quench of a REBCO tape for two cases; (a)  $I_{op} = 70\text{ A}$  and normal-zone length = 1 m and (b)  $I_{op} = 130\text{ A}$  and normal-zone length = 10 m (where normal-zone length is the length of tape operated in normal mode).

tention. As shown in Fig. 7 (b), however, the maximum voltage in the coil is  $\sim 6\text{ V}$ , which is under the acceptable level for a polyimide-wrapped REBCO tape.

Since the one-turn length of the REBCO tape is around 1 m, the heat generated at the hot spot must be dispersed into several layers in the winding pack. Generally, the heat from the hot spot transfers only along the REBCO tape through the copper laminate, and should be precluded in the direction of the adjacent layers because of the poor heat conductivity of the Hastelloy substrate. Consequently, to improve heat transfer between adjacent layers of the REBCO tape, we inserted 0.8 mm-thick heat transfer plates made of pure aluminum sheet between a coil frame and winding pack at the top and bottom sides, as shown in Fig. 2. This plate would enable heat dispersion to adjacent layers. Such heat transfer is facilitated at the top/bottom areas of the winding pack by the magnetic field being maximized, while the heat transfer plate cannot be placed in other areas because of the layer-winding.

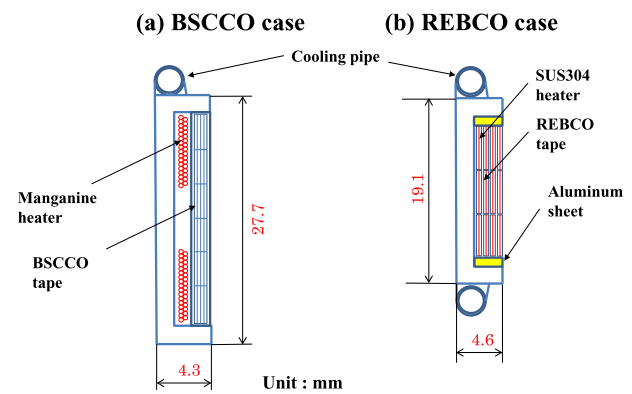


Fig. 8 Schematics of PCSs made from (a) BSCCO tape and (b) REBCO tape.

### 2.3 Design of a PCS with a REBCO tape

The designed PCS was expected to act as a damping resistor to protect the main coil, in addition to its switching function. Hence, the PCS was introduced as an HTS tape winding into the Mini-RT device. At very large magnetic energies, a larger PCS might be required, whose temperature would be more difficult to control. Therefore, a thin  $\text{YBa}_2\text{Cu}_3\text{O}_{7-\delta}$  film with a heater was employed in the RT-1 device [13], yielding a switching time of around 1 min. However, to enable damping of the magnetic energy in the main coil, the resistor was installed inside the internal coil in the RT-1 device.

Here, to prevent unnecessary magnetic fields, the tape was wound using a bifilar method. In the BSCCO PCS, a manganese heater was employed, as shown in Fig. 8 (a). Although this BSCCO coil sufficiently performs the basic function of the PCS, its operation introduces some problems; namely, a large temperature difference establishes along the BSCCO tape (e.g.,  $\Delta T = 20\text{--}30\text{ K}$ ), and heating and cooling of the PCS consumes a relatively long time (e.g., 5–10 min). The new PCS employing the REBCO tape was designed to alleviate these problems. For comparison, the specifications of the REBCO PCS and BSCCO PCS are listed in Table 3.

The REBCO PCS achieves the following improvements:

- (1) reduction of PCS size,
- (2) introduction of a sheet-type heater made from a stainless steel,
- (3) equipment of cooling pipes on both sides of the PCS winding frame,
- (4) insertion of a heat transfer plate between the winding pack and frame.

The length of the REBCO tape was  $\sim 22\text{ m}$ , which is determined by considering the energy damping reservoir of the main coil. As shown in Fig. 6, even if the REBCO PCS consumes the total magnetic energy stored in the main coil, also the increase in temperature is small enough ( $\Delta T = 30\text{--}$

Table 3 Specification of the PCS made from BSCCO and REBCO tapes. The BSCCO PCS was recently replaced with the REBCO PCS.

	BSCCO PCS	REBCO PCS
Super conductor	Ag (5%Au)-sheathed Bi-2223	REBCO
Size of the PCS		
Inner diameter	326.8 mm	329.8 mm
Outer diameter	335.4 mm	335 mm
Height	23.7 mm	13.8 mm
Total turns and winding	20 turns, bi-filer	22 turns, bi-filer
Heater	Manganese $\phi = 0.5$ mm	SUS304L (10 $\mu\text{m} \times 4.3$ mm)
total resistance at R.T.	202 $\Omega$	440 $\Omega$
heating power	50 W	50 W
operation current/voltage	0.5A/101V	0.34A/148 V
Total weight	0.9 kg	0.71 kg

Table 4 Heat transfer rates through current leads for the Ag (5% Au)-sheathed BSCCO tape and the REBCO tape.

	BSCCO	REBCO
Super conductor	Ag (5%Au)-sheathed Bi-2232	REBCO
Critical current: $I_c$ at 77K, self-field, 1 $\mu\text{V}/\text{cm}$	$\sim 220$ A	216 - 223 A
Size of the conductor	4.3 mm $\times$ 0.23 mm	4.0 mm $\times$ 0.1 mm
Cross section of heat transfer	4.3 mm $\times$ 0.23 mm $\times$ 1.6/2.6* = 0.61 mm <sup>2</sup>	4.0 mm $\times$ 0.008 mm** = 0.032 mm <sup>2</sup>
Total length of the current lead	300 mm	
Heat transfer rate	0.0073 W	0.0079 W

\*) Only the silver area is considered.

\*\*) Only the silver layer is considered.

40 K). Although the total length of the HTS tape was comparable between the BSCCO and REBCO PCSs, the total weight of the REBCO PCS was reduced to be 0.71 kg, compared with 0.9 kg for the BSCCO PCS. This weight reduction improved the thermal response of the REBCO PCS. In the BSCCO PCS, since a manganese heater was wound behind the BSCCO tape, the tape was heated from only one side, as shown in Fig. 8 (a). Such nonhomogeneous heating might account for the nonuniform temperature of the BSCCO tape ( $\Delta T = 20$ -30 K). To avoid this problem, a 0.01 mm-thick stainless steel sheet was wound together with the REBCO tape, as shown in Fig. 8 (b). Thus, the temperature difference in the PCS was now reduced ( $\Delta T = 5$ -10 K). The total resistance of the stainless steel sheet was 440 $\Omega$ . To excite the coil current, the PCS was typically heated to 95 K. A heating power of  $\sim 20$  W was required to heat the PCS to 95 K in 5 min. Once the main coil is excited, the PCS should be cooled as rapidly as possible, because quenching the current lead (i.e., the BSCCO tape) would be afraid in the Mini-RT device. Thus, a cooling pipe was added at the bottom of the PCS, as shown in Fig. 8 (b). Finally, to improve the heat conduction between the PCS layers, the aluminum heat transfer plate was in-

serted, as shown in Fig. 8 (b).

## 2.4 Overall design of the persistent current circuit

In the BSCCO coil, to minimize the heat ingress from the external electrode to the main coil and the PCS, a silver (5% Au)-sheathed BSCCO tape was employed for the current lead, which was connected to the external power supply. This is because the heat conductivity of the silver (5% Au)-sheathed BSCCO tape is about 10 times lower than that of pure silver-sheathed BSCCO tape. To further reduce heat ingress, the external electrode was cooled with liquid nitrogen. Hence, by implementing these designs, we successfully excited the main coil to the rated current ( $I_{op} = 120$  A in the BSCCO coil). In this study, we have also considered the possibility of the current lead with the REBCO tape. The characteristics of the silver (5% Au)-sheathed BSCCO and REBCO tapes are compared in Table 4. Since the heat conductivity of both tapes is similar, we adopted the silver (5% Au)-sheathed BSCCO tape as the current lead, because this tape is potentially more tolerant to tape burnout.

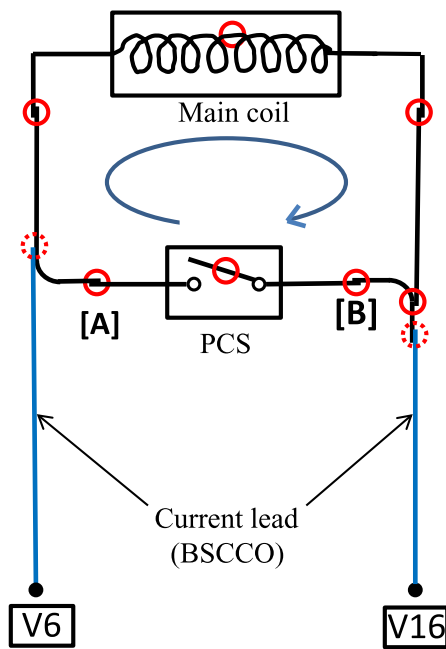


Fig. 9 Schematic of the persistent current circuit. The main coil and the PCS are made from REBCO tapes, and the current lead to the external power supply is a silver (5% Au)-sheathed BSCCO lead. The joint sections are represented by the overlapping of the tapes (marked with red circles). During persistent current operation, the joint sections (marked with solid red circles) contribute to the resistance in the persistent current electric circuit. Since joint sections exist inside the main coil and PCS, seven joint sections are present in the persistent current operation. The voltages at the joint sections (A) and (B) were directly measured, as shown in Fig. 21.

Figure 9 is a circuit diagram of the REBCO coil. Intrinsically, a single joint section exists in the main coil, marking the connection of two ~300 m-long REBCO tapes. In the PCS, another joint section exists at the starting point of the bifilar winding. Several additional joint sections of the REBCO tape are present in the persistent current circuit, because the main coil, PCS, and current leads to the electrodes for the external power supply should be interconnected. To join the REBCO tapes for overcoming the high electric resistance of the Hastelloy, the copper laminate sides are turned toward each other and soldered together, as shown in Fig. 10.

To reduce the electrical resistance, the joint region should be extended as far as possible. However, a uniform solder joint over long regions presents a technical difficulty. To examine the characteristics of the solder joint between two REBCO tapes, we measured the joint resistance at different joint lengths (10 mm, 20 mm, 30 mm, and 50 mm). As shown in Fig. 11, the joint resistance decreased with increasing joint length, and saturated around 30 mm. Since a current decay of <1% during a few hours is acceptable for plasma experiments, a joint resistance be-

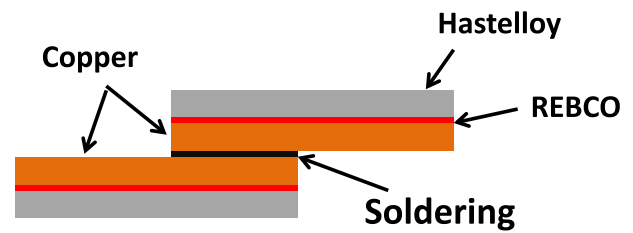


Fig. 10 Schematic of the joint section between two REBCO tapes, where the copper laminates were jointed with solder over a 30 mm length.

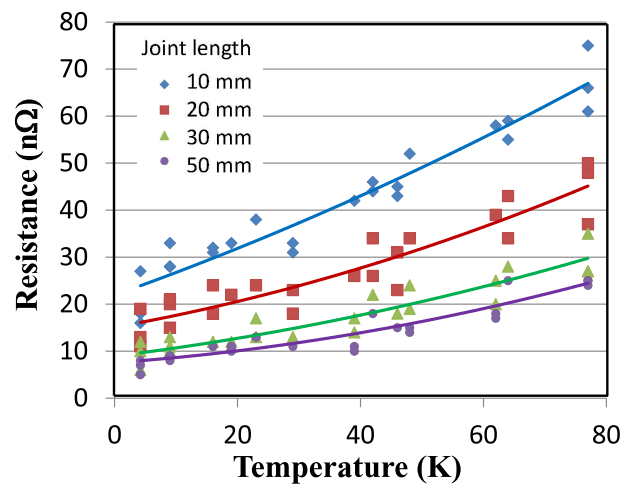


Fig. 11 Joint resistance as a function of tape temperature for different joint lengths.

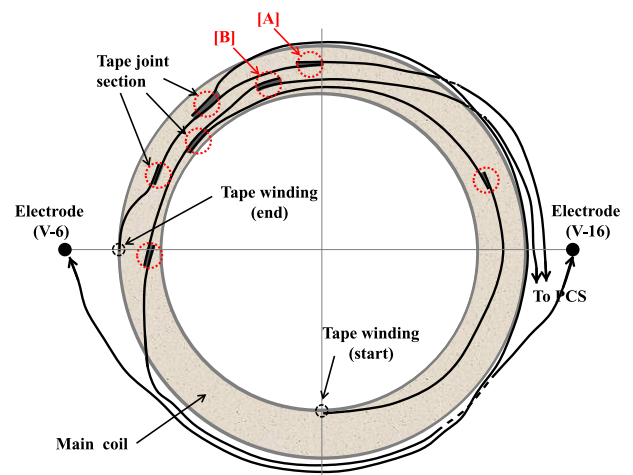


Fig. 12 Top view of the winding pack of the Mini-RT coil, and distribution of the REBCO/BSCCO tape leads. Red broken circles indicate the joint sections where two tapes overlap. The joint sections (A) and (B) in Fig. 9 are also highlighted.

low 20 - 30 nΩ might be sufficient. Moreover, considering the technical reliability of the solder joint, we specified the joint length as 30 mm.

Figure 12 shows the layout of the REBCO tapes connected to the main coil, PCS, and interconnecting current leads. The connecting HTS tapes were located at the ceiling of the coil frame, and cooled by the main coil. While connecting the REBCO tape, we must ensure that (a) the copper sides of two REBCO tapes turn toward each other, and (b) the REBCO tape can't be twisted, because the Hastelloy substrate is quite stiff for twisting. Instead of twisting REBCO tape, an additional short piece of REBCO tape was inserted, as shown in Fig. 12. Despite the simplicity of the electrical circuit shown in Fig. 9, the layout of the REBCO tape appears quite complicated. As shown in Figs. 9 and 12, seven joint sections were ultimately required along the persistent current circuit. The combined resistance of these joint sections is possibly responsible for the decline in persistent current.

### 2.5 Fabrication of the Mini-RT coil

Initially, having fabricated the main coil and the PCS, we constructed the electrical circuit of the persistent current. The performance of this persistent current coil system was experimentally tested in the cryostat. Figure 13 shows photograph of the experimental set-up. The system was cooled to 35 K, and the current persisted at its rated current of 100 A. Details of this experiment are provided in [14].

Next, the winding pack of the main coil and the PCS constructed from BSCCO tapes in the Mini-RT coil were replaced with their REBCO counterparts. The current lead comprising the silver (5% Au)-sheathed BSCCO tape was connected to the newly fabricated REBCO coil system. Almost all of the connecting tapes were located at the coil frame, while the current lead was not supported during the length of ~300 mm, so as to prevent heat leakage and/or input between the electrode and the coil.

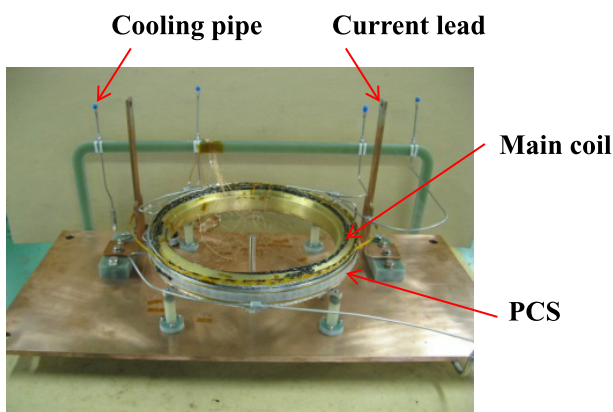


Fig. 13 Photograph of the winding pack of the main coil and the PCS. This system was tested with a cryostat to reconfirm the characteristics of the persistent current mode.

## 3. Excitation Experiments

### 3.1 Cooling characteristics and heat leakage of the REBCO coil

The internal coil was cooled with He gas supplied by two GM refrigerators (combined power 33 W at 20 K). The layout of cooling pipes in the internal coil is shown in Fig. 14. The cold He gas inside the internal coil is guided through the inlet transfer tube, and separately distributed to the main coil and the PCS.

The superconducting characteristics of the REBCO tape are sometimes degraded during REBCO coil fabrication [15]. Peeling of the REBCO layer is considered to contribute to this deterioration. Since the REBCO layer attached to the substrate is extremely thin (typically 1 - 2 μm), the critical stress of the REBCO layer against the peeling force is quite low (typically several tens of MPa). When the winding pack of the REBCO coil is stiffly packed with resins, the peeling force can be introduced by thermal stress during the cooling of the REBCO coil. To alleviate thermal stress, slow cooling of the REBCO coil might be preferable, because it prevents nonuniform shrinkage of the REBCO coil during the cooling process. In the current experiments, we applied a cooling rate of ~10 K/h. Figure 15 shows a typical cooling history of the main coil and the PCS, in which a single GM refrigerator was employed

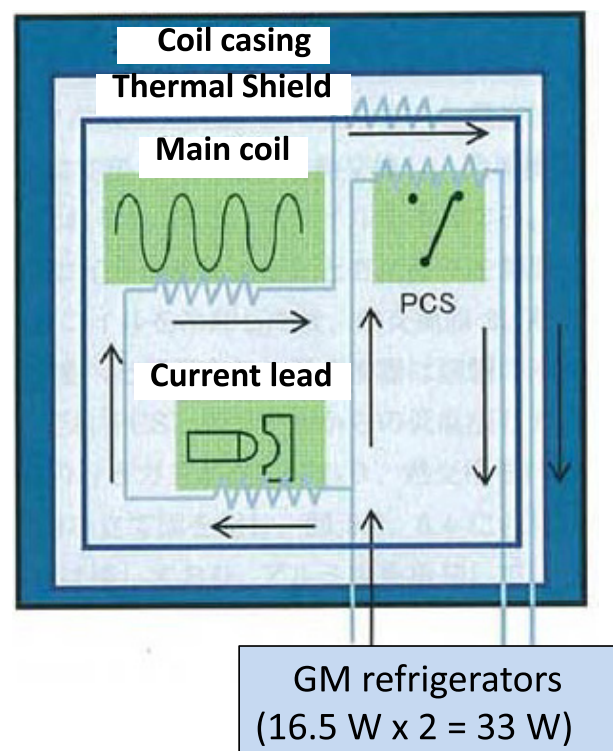


Fig. 14 Cooling system of the Mini-RT coil, comprising two GM refrigerators. Note the single inlet and two outlets. When the PCS is heated to ~100 K to maintain the switch-off condition, the cooling channel at the PCS side is closed.

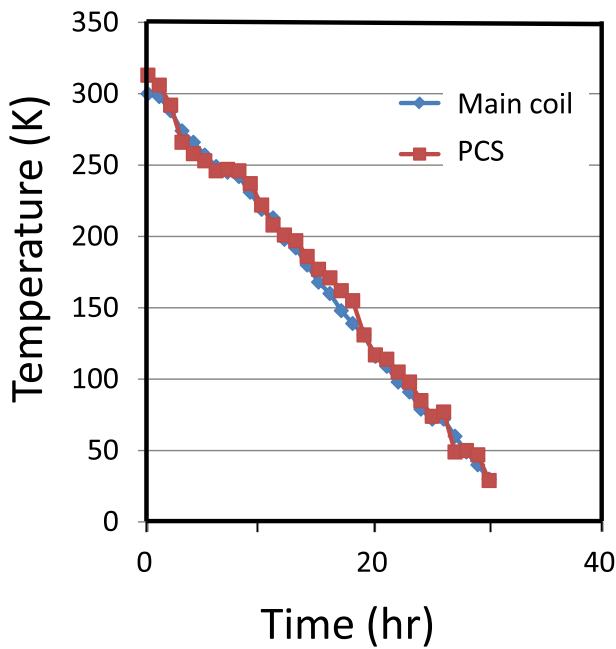


Fig. 15 Behavior of the REBCO coil as it is cooled from room temperature to 25 K. The cooling rate of  $\sim 10$  K/h is achieved by controlling the flow rate of the cold He gas.

during the initial phase and the cooling rate was controlled by altering the flow rate of the cold He gas. This cooling system decreased the temperature of the REBCO coil to around 25 K.

We next examined the heat input to the main coil. No cooling system is applied during the plasma operation (in other words, during persistent current operation). Therefore, the duration of plasma experiments is limited by the temperature increase of the internal coil. The temporal temperature rise in the main coil and the PCS in the absence of the cooling system is plotted in Fig. 16. Temperature data are lacking in the plasma experiment phase, during which the coil temperature was not measured. At the completion of a plasma experiment, typical coil temperature was 50 - 60 K.

From this temperature increase of the main coil, the estimated heat input to the main coil was about 2.4 W. The source of this heat input to the main coil might be radiation from the thermal shield ( $\sim 1$  W), and heat conduction from fixtures such as the coil support ( $\sim 0.25$  W), cooling pipe ( $\sim 0.2$  W), current lead ( $\sim 0.05$  W), and diagnostic cables ( $\sim 0.05$  W). The main coil and the PCS were wrapped in five layers of multi-layer insulation (MLI). Since the effectiveness of thermal shielding might depend on the performance of MLI, we suspect that heat input to the coil is predominantly in the form of radiation through the MLI from the thermal shield.

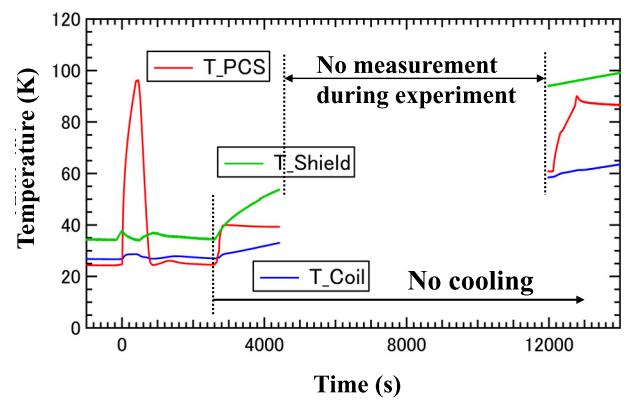


Fig. 16 Natural rise of the REBCO coil temperature in the absence of active cooling. The cooling of the main coil, PCS, and shield was stopped at  $t = 2600$  s, and temperatures begin to increase because active cooling was no longer maintained.

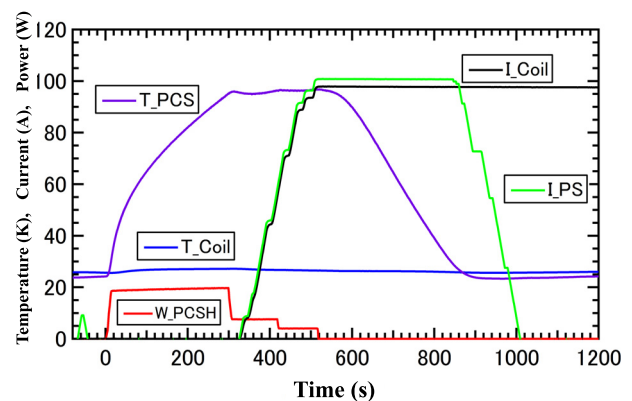


Fig. 17 Excitation experiment of the REBCO coil. Initially, the temperature of the PCS increases with heating of the PCS, and the main coil current is excited by the external power supply. Next, the PCS is cooled and the external current declines, thereby establishing the persistent current.

### 3.2 Excitation of the main coil and operation of the persistent current mode

The excitation scenario of the REBCO and BSCCO coil systems is identical. Typical temporal behavior of the coil parameters is plotted in Fig. 17. Immediately following PCS cooling, the PCS heater was switched on. When the PCS temperature reached  $\sim 95$  K, the power supplied to the heater was reduced sufficiently such that temperature did not increase further. Having established the switch-off condition of the PCS, the main coil was excited by the external power supply to its rated operation current at a ramp-up rate of 1 A/s. Once the main coil had reached the rated current, the PCS was rapidly cooled. Typically, the PCS reaches  $\sim 30$  K within a few minutes. Finally, the current of the external power supply was reduced to zero, and the persistent current in the circuit of the main coil and the

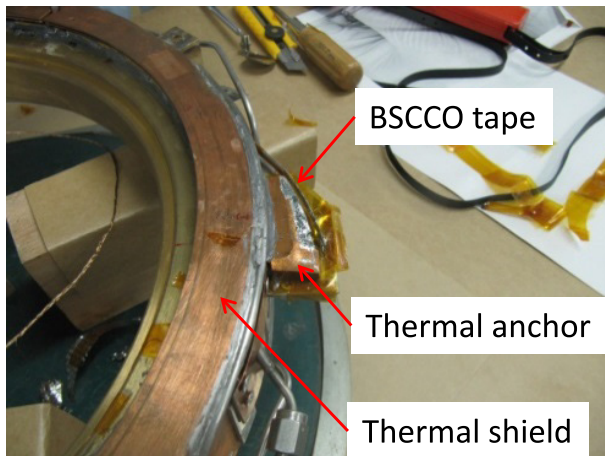


Fig. 18 Photograph of the thermal anchor of the current lead. The silver (5%Au)-sheathed BSCCO tape is connected to the thermal shield through a thermal anchor fabricated from a copper block.

PCS was established. Since the temperatures of the main coil and PCS were slightly increased by the heat input to the PCS, it took several minutes to cool the REBCO coil system. Once the main coil and the PCS were sufficiently cooled, the transfer tubes were detached from the coil, and the internal coil was mechanically lifted to the mid-plane of the vacuum vessel for the plasma experiments.

### 3.3 Demagnetization of the main coil

Immediately following plasma experiments, the main coil must be demagnetized. At first, we tried to reverse the excitation process in the internal coil. The external electrodes cooled by liquid nitrogen were inserted into the coil, and the current of the external power supply was increased to the rated coil current. However, the quenching occurred at the current lead constructed from the BSCCO tape, because this current lead is connected to the thermal shield, as shown in Fig. 18. The excitation phase requires this thermal anchor, since cooling of the current lead is reinforced by the cooled (to  $\sim 30$  K) thermal shield. In contrast, during the demagnetization phase, the temperature of the thermal shield might increase to around 100 K (see Fig. 16).

Notably, during demagnetization, the temperature of the transfer tube might increase to room temperature approximately. In addition, no by-pass cooling channel is installed in the Mini-RT device (see Fig. 14). If the transfer tube is connected to the main coil, the He gas heated by the transfer tube would be transferred to the main coil and PCS. Therefore, to avoid this thermal shock, we do not re-cool the internal coil during demagnetization. Consequently, the reverse excitation process was not applicable in the Mini-RT coil, since temperature of the current lead can approach the critical temperature of the BSCCO tape; moreover, the coil was not equipped with a damping resistor. Thus, demagnetization of the Mini-RT coil was

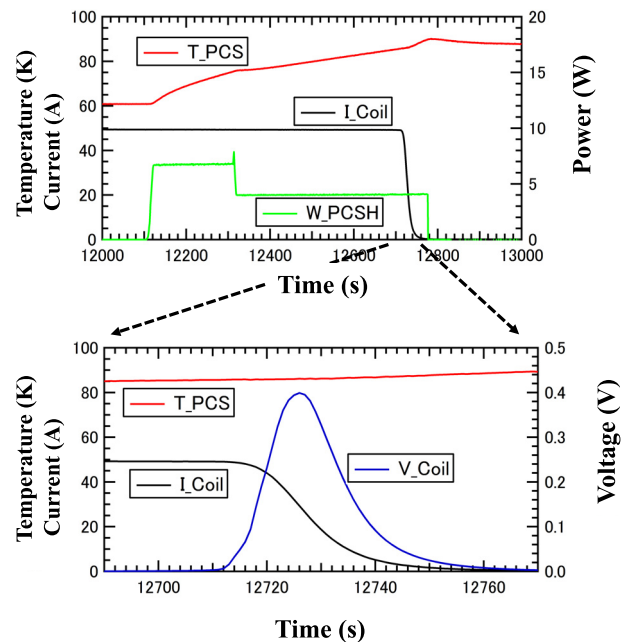


Fig. 19 Temporal behaviors of the coil parameters during the demagnetization phase. The PCS temperature gradually increases, and current decay begins at the time of super-normal transition of the PCS. The temperature increase of the PCS and the induced voltage across the main circuit are also shown.

achieved via the PCS, which was designed to safely consume the stored magnetic energy of the main coil.

Figure 19 shows the temporal evolutions of the coil parameters during the demagnetization phase. Initially, the PCS heater was switched on, and the temperature gradually increased. When the PCS temperature reached the critical temperature of the REBCO tape ( $\sim 85$  K), the persistent current was decayed by the emergent PCS resistance. The time constant of the persistent current decay was around 7 - 8 s, and the induced voltage across the circuit was at most 0.4 V. Since the resistance during the demagnetization phase was calculated as  $\sim 20 \Omega$ , the estimated length of the normal transition zone of the REBCO tape in the PCS was 1 - 1.5 m. While, in the case of demagnetization at 10 A persistent current, the current decay time was prolonged ( $\tau \sim 30$  s). Therefore, we deduce that the normal transition zone lengthens as the operation current is increased. As shown in Fig. 19, the PCS temperature slightly increased as the device absorbed magnetic energy. The temperature increase in the PCS can be evaluated, as shown in Fig. 6. At an operation current of 50 A, the estimated maximum temperature was 170 K; in contrast, the experimental data shows a maximum temperature of roughly 90 K, possibly because heat was dispersed through other heat channels.

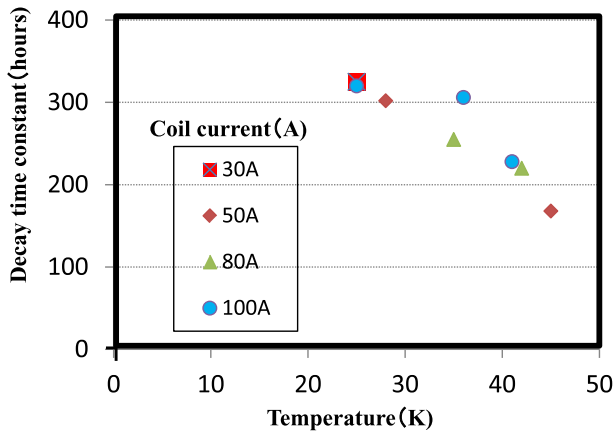


Fig. 20 Decay time constant of the persistent current for various coil currents as a function of the coil temperature. The decay time depends on the coil temperature, but is independent on coil current.

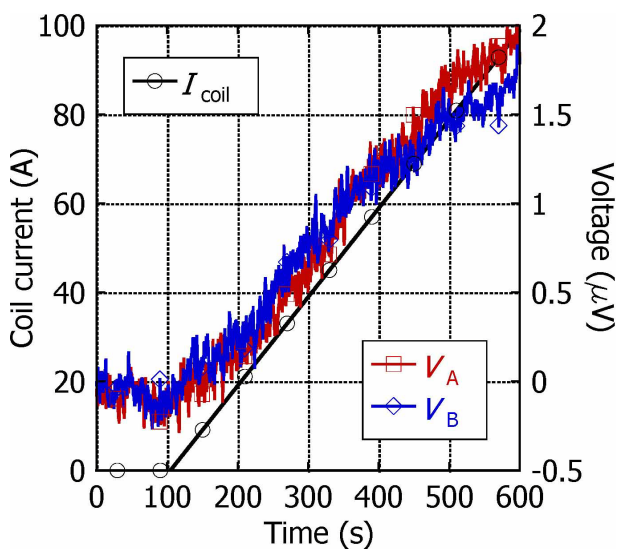


Fig. 21 Measured voltages across the joint sections (A) and (B) in Fig. 9. The coil current is ramped up to 100 A at  $T_{\text{coil}} = 41$  K.

### 3.4 Decay time constant of the persistent current

The resistance in the circuit of the main coil and the PCS induces gradual decline in the persistent current. Figure 20 shows the e-fold time of the current decay measured for various coil currents at different coil temperatures. At 25 K, the decay time was independent of operating current and exceeded 300 h, corresponding to a resistance of  $\sim 125$  n $\Omega$  in the persistent current circuit. Possible causes of the resistance include flux flow loss, contact resistance at the joint sections and defects on the tape introduced during fabrication, and/or cooling of the REBCO coil. The persistent current circuit contains seven joint sections (see Fig. 9). Since the joint resistance at a single section is  $\sim 15$  n $\Omega$  at 25 - 30 K (see Fig. 11), the overall joint

resistance is estimated to be 100 - 110 n $\Omega$ . We measured the voltages induced across the joint regions at 41 K using the voltage taps shown in Fig. 9. The voltages across the joints (A) and (B) in Fig. 9 are presented in Fig. 21, where the coil current was 100 A. The measured voltages (electrical resistances) across (A) and (B) were 2  $\mu\text{V}$  (20 n $\Omega$ ) and 1.5  $\mu\text{V}$  (15 n $\Omega$ ), respectively, consistent with the data shown in Fig. 11. The decay time of the persistent current also depends on the temperature, consistent with data of joint resistance shown in Fig. 11. Thus, we conclude that the decay time of the persistent current is primarily determined by joint resistance, and that fabrication and cooling introduce no serious defects onto the REBCO tape.

## 4. Summary

In 2003, an HTS coil fabricated from BSCCO was adopted as the internal floating coil of the plasma experimental device Mini-RT, which has been extensively used in plasma experiments. The decay time constant of the persistent current in this device was 20 - 30 hours, which was considerably shorter than expected, and possibly degraded by defects introduced during the fabrication process. During 10 years of operation, the current decay of the persistent current has gradually fallen to  $\sim 2.7$  h. Such deterioration is problematic for plasma experiments, where a constant magnetic field is preferable.

The production of REBCO tapes and coils has advanced sufficiently for us to consider replacing the BSCCO coil with a new REBCO coil in the Mini-RT device. In this study, the REBCO tape was 4.3 mm wide, and the total current in the fabricated REBCO coil was 55.2 kA. As for the countermeasure on the quench, a 0.1 mm-thick copper laminate was attached, and the coil was electrically insulated by a polyimide sheet. The final thickness of the REBCO tape was 0.27 - 0.28 mm. If a few meters of the REBCO tape would be transitioned into the normal conducting state at the quench, the temperature of the REBCO tape should not exceed 200 K. Thus, to improve the heat dispersion at hot spots, an aluminum sheet was inserted between the winding pack and the coil frame. A persistent current switch was fabricated from the REBCO tape, and several improvements were introduced. As a uniform heating source, a stainless steel sheet was wound together with the REBCO tape. In addition, the cooling system was reinforced by an additional cooling channel. The size of the PCS was determined from its role as a heat sink for the stored magnetic energy during the demagnetization phase. The REBCO tapes were joined by a wrap-joint soldered at the copper laminate sides. In preliminary development, 30 mm was decided as the joint length. Notably, joint resistance depends on both joint length and tape temperature.

To prevent thermal stress induced by nonuniform contraction of the main coil, the coil and PCS were gradually cooled from room temperature to 25 K at  $\sim 10$  K/h. Using the PCS and an external power supply, the current of the

main coil was excited, and a persistent current was established. Under operation at 25 K, the decay time of the persistent current was improved to 320 h. The corresponding resistance was 125 n $\Omega$ , which is comparable with the total resistance of the seven joint sections in the persistent current circuit. The decay time was observed to reduce with increasing operation temperature. Based on these observations, we infer that the decay constant of the persistent current is attributable to joint resistance, and that the REBCO tape was not seriously degraded during the fabrication and cooling process.

## Acknowledgments

The authors acknowledge Fuji Electric Co., Ltd. for the fabrication of the REBCO coil and Fujikura Co. for the supply of the REBCO tape. This study was supported by a Grant-in-Aid for Scientific Research (No. 23360410) from the Ministry of Education, Culture, Sports and Technology, Japan. This study was performed with the support and under the auspices of the National Institute for Fusion

Science (NIFS) LHD Project Research Collaboration Program (NIFS11K0BA024).

- [1] Y. Ogawa *et al.*, J. Plasma Fusion Res. **79**, 643 (2003).
- [2] T. Mito *et al.*, IEEE Trans. Appl. Supercond. **13**, 1500 (2003).
- [3] N. Yanagi *et al.*, IEEE Trans. Appl. Supercond. **13**, 1504 (2003).
- [4] Y. Ogawa *et al.*, J. Cryo. Soc. Jpn. **39**, 175 (2004).
- [5] T. Mito *et al.*, J. Cryo. Soc. Jpn. **39**, 182 (2004).
- [6] N. Yanagi *et al.*, J. Cryo. Soc. Jpn. **39**, 193 (2004).
- [7] N. Yanagi *et al.*, J. Cryo. Soc. Jpn. **39**, 201 (2004).
- [8] J. Morikawa *et al.*, J. Cryo. Soc. Jpn. **39**, 209 (2004).
- [9] Y. Ogawa *et al.*, Fusion Eng. Des. **81**, 2361 (2006).
- [10] M. Kikuchi *et al.*, SEI Technical Review **172**, 71 (2008).
- [11] R. Freeman *et al.*, IAEA-CN-28/A-3 (Madison) (1971).
- [12] O.A. Anderson *et al.*, IAEA-CN-28/A-8 (Madison) (1971).
- [13] Y. Ogawa *et al.*, Plasma Fusion Res. **4**, 020 (2009).
- [14] K. Natsume *et al.*, Applied Superconductivity, IEEE Transactions, vol.24, 4601104 (2014).
- [15] Y. Yanagisawa and H. Maeda, J. of Cryogenics and Superconductivity Society of Japan **48**, 151 (2013).